JOURNAL OF CATALYSIS 157, 25–34 (1995)

The Impact of Aqueous Impregnation on the Properties of Prereduced vs Precalcined Co/SiO_2

George J. Haddad and James G. Goodwin, Jr.[1]

Department of Chemical and Petroleum Engineering, University of Pittsburgh, Pittsburgh, Pennsylvania 15261

Received August 9, 1994; revised June 13, 1995; accepted July 14, 1995

One of the methods of preparing model supported metal catalysts for fundamental studies of promoter effects is by sequential impregnation of reduced catalysts. In general, such promotion has been found not to alter the metal particle size distribution. However, the promotion process itself may possibly result in chemical and/or structural modifications of certain catalysts. In order to better understand how the process of promotion may itself modify a Co catalyst, the effect of water impregnation and drying at various temperatures (25–110°C) of reduced or calcined 20% Co/SiO_2 was investigated. The results show that water impregnation and subsequent drying had a significant effect on the structure of the *reduced and passivated* Co catalysts. The Co oxide phase declined in favor of a Co silicate/hydrosilicate phase which reduced completely only above 800°C. Steady-state isotopic transient kinetic studies of ethane hydrogenolysis revealed that the surface concentration of reaction intermediates declined following water impregnation, which suggests that the Co silicate/hydrosilicate formed was inactive. Aqueous impregnation and drying of *calcined* Co/SiO_2, on the other hand, did not appear to modify the catalyst in any significant way. © 1995 Academic Press, Inc.

INTRODUCTION

The process of adding a chemical promoter to a metal catalyst is a complicated one and could result in chemical and/or physical modifications of the metal catalyst itself, which would obscure the effect of the promoter on the catalytic properties. One of the methods of adding a promoter to a metal catalyst in more fundamental studies of promoter effects is by sequential impregnation. The impregnation of the catalyst support with the solution of the metal compound is done first, followed by calcination and/or reduction to produce a "base" catalyst. The promoter is then added by a secondary impregnation. In a number of cases, this has been found not to alter the metal particle size distribution (1, 2). Effects due to variations in metal particle size and distribution are, therefore, technically avoided, and any change in catalytic properties is assumed to be due primarily to promoter effects alone. However, little research has addressed how this promotion process itself may possibly result in chemical and/or structural modifications of certain catalysts.

It is well known that Co is one of the most active metals for Fischer–Tropsch synthesis (FTS) and well suited for the production of high molecular weight waxes. Promoters, such as K and La, are routinely added in order to increase the chain growth probability during FTS (3, 4). One catalyst system of particular interest is based on Co/SiO_2 (5, 6).

Ethane hydrogenolysis is a highly structure-sensitive reaction (7–9) requiring for a reaction site a large ensemble of metal atoms (9). The reaction rate depends heavily on the metal crystal size (10) and on the type of crystal faces exposed (9). Thus, it has been found to be useful to explore structural changes in supported metal catalysts as a result of support effects (11), calcination/reduction (12), and the presence of modifiers (8, 9, 13).

This paper reports the results of an investigation of modifications of a 20% Co/SiO_2 catalyst during secondary aqueous impregnation and drying. The findings reported here help us to understand better the variability/inconsistency of results from different promotion studies in the literature.

EXPERIMENTATION

Catalyst Preparation

Catalyst nomenclature. In this paper, catalyst designation is given by B*X*-RP(or C)-W*Y*-*T*, where "B" refers to the calcined, reduced, and passivated 20% Co/SiO_2 base catalyst; "*X*" to the pH of cobalt precursor solution; "RP" to reduction, and passivation; "C" to recalcination; "W" to a second water impregnation at a pH of "*Y*"; and "*T*" to the temperature (in °C) of drying following water impregnation.

Preparation of base Co catalysts. The 20% Co/SiO_2 base catalysts were prepared by the incipient wetness technique using an aqueous solution of $Co(NO_3)_2 \cdot 6H_2O$ (J. T. Baker Inc.) and Cab-O-Sil silica (amorphous fumed

[1] To whom correspondence should be addressed.

0021-9517/95 $12.00
Copyright © 1995 by Academic Press, Inc.
All rights of reproduction in any form reserved.

silica powder from Cabot Corp.). The solution pH used was 4.5 or 5. Incipient wetness occurred at about 1.8 ml/g of silica. Impregnation was followed by drying at 90° overnight, calcining at 300°C for 6 h, and reducing under H_2 at 350°C for 22 h. Temperature ramp rates used during calcination and reduction were 1°C/min. The catalysts were passivated after reduction by allowing air to leak slowly into the reduction chamber.

Preparation of water-impregnated Co catalysts. Catalysts B4.5-RP-W6-25, B4.5-RP-W6-50, B4.5-RP-W6-90, and B4.5-RP-W6-110 were obtained by impregnating the reduced–passivated B4.5-RP base catalyst with distilled water of pH 6 followed by drying overnight at 25, 50, 90, or 110°C. Drying at 25°C was performed under vacuum to ensure adequate moisture removal. Catalyst B5-C-W6-90 was prepared by recalcining the prereduced B5-RP catalyst in air at 300°C for 5 h before impregnating it with distilled water of pH 6 and drying at 90°C overnight.

Elemental Analysis

Elemental analysis using inductively coupled plasma spectroscopy (ICP) (Galbraith Laboratories) was carried out to determine final Co loadings. ICP was also done on the water phase of a (20% Co/SiO_2 + water) slurry heated at 90°C for 12 h to investigate any leaching of contaminants from the silica to the solution during the drying step of the catalyst preparation.

BET

Nitrogen sorption at 77 K (Pittsburgh Applied Research Corp.) was used to obtain the BET surface area of the catalysts. BET was also performed on the catalysts to determine any structural changes to the silica (a) after Co precursor solution impregnation, drying, calcination, reduction, and passivation and (b) after a second aqueous impregnation of the reduced and passivated catalyst and drying.

XRD Measurements

X-ray measurements were performed on a Philips X'pert System X-ray diffractometer with monochromatized CuK_α radiation. The XRD instrument was operated at 40 kV and 30 mA. Three hundred mg of each catalyst was placed inside a dish for XRD. Using the same amounts for all the catalysts allowed for quantitative analysis to be carried out on the XRD profiles. The spectra were scanned at a rate of 2.4°/min (in 2θ).

Static Hydrogen Chemisorption

Gas volumetric chemisorption was determined according to the method of Reuel and Bartholomew (14). The catalyst was first heated in 100 cc/min of H_2 to 320°C at a rate of 1.6°C/min and then held at this temperature for 12 h in order to rereduce it. H_2 was then desorbed for 1 h at 320°C under a vacuum of 10^{-6} Torr. After H_2 chemisorption for 5 h at 100°C with an initial H_2 pressure of 350 Torr, the adsorption isotherms were measured at 25°C by the decreasing pressure method. The high temperature for initial adsorption was used since the chemisorption process is known to be highly activated on cobalt (15). One hour was allowed for equilibration at each H_2 pressure at 25°C. The amount of total chemisorption was obtained by extrapolating the total adsorption isotherm to zero pressure. The reversible H_2 desorption isotherm was measured at 25°C following evacuation of the catalyst for 10 min at that temperature. The total amount of chemisorbed H atoms was used to determine the number of vacant Co^0 atoms at the surface using the relationship $H/Co_s = 1$ (14).

Temperature-Programmed Reduction

TPR experiments were conducted on the Co catalyst using an Altamira Instruments AMI-1. A catalyst was reoxidized by flowing ultrapure O_2 over it while heating at a ramp rate of 5°C/min to 350°C. This temperature was maintained for 6 h to ensure complete oxidation; then the temperature was brought down to 40°C while still under O_2 flow. In order to flush the gas phase and any weakly adsorbed O_2 on the catalyst from the system, Ar was allowed to flow through the catalyst at 40°C for 1/2 h. A 5% H_2 in Ar gas mixture (Matheson) was used as the reducing gas with a flow rate of 30 cc/min and a temperature ramp of 5°C/min to 900°C. The amount of H_2 consumed by the catalyst was detected using a thermal conductivity detector (TCD) and recorded as a function of temperature.

Ethane Hydrogenolysis

The experimental setup for this reaction was a differentially operated, fixed-bed Pyrex reactor. A gas mixture of 10% ethane in H_2 (Linde, CP grade) was used without any further purification. Additional H_2 (Liquid Carbonic Specialty Gas Corp., Ultra Pure) for the reaction was further purified by passing through a Deoxo unit and an activated charcoal trap. He (Liquid Carbonic Specialty Gas Corp., Ultra Pure, 99.999%) was used as a diluent after passing through a molecular sieve trap. Brooks mass flow controllers were used to control the flow of gases. A catalyst was first heated in 100 cc/min of H_2 to 320°C at a rate of 1.6°C/min and then held at this temperature for 12 h in order to rereduce it. A temperature of 320°C for rereduction was used instead of the original 350°C reduction temperature in order to minimize any thermal modifications to the catalyst. The flow rates used for the reaction were $H_2/C_2H_6/He$ = 15/0.3/84.7 cc/min at 101 kPa pressure. A six-way valve was used to switch between the reaction mixture and H_2 flows. Reaction temperatures and flow

rates were selected to give conversions of less than 5% for catalyst samples of 35 mg.

In order to study the initial reaction on a clean catalyst with minimal deposited carbon, product stream analysis was done after 5 min of reaction. The catalyst was then bracketed with H_2 for 30 min at reaction temperature. This was shown to effectively restore the initial activity of the catalyst. The data for the Arrhenius plots were obtained by taking the first reaction measurement at 280°C, the highest reaction temperature used in this study. The rest of the reaction data were then taken at lower temperatures in 20° intervals with hydrogen bracketing between reaction measurements. After measurement at the lowest temperature, the temperature was increased to the initial temperature of 280°C and the activity remeasured to ensure that the catalyst had not undergone any significant change. Product analysis was performed using a Perkin–Elmer 8500 gas chromatograph fitted with a porapack-Q column and a flame ionization detector (FID) and held at 90°C.

Isotopic Transient Kinetics during Ethane Hydrogenolysis

Steady-state isotopic transient kinetic analysis (SSITKA), developed in large part by Happel (16) and Biloen (17), is a powerful kinetic technique for studying catalyst surfaces under reaction conditions. By using isotopic transients and keeping a constant reaction environment during the analysis, accurate measurements of the concentration of intermediates and their activities are possible during steady-state reaction. This technique was performed as described elsewhere (18). From these results, one can better assess the effect of catalyst pretreatment.

RESULTS

Effect of Preparation Steps on the Support

The surface area of the silica was determined to be 184 m^2/g by BET. On one hand, BET surface measurements indicated no significant alteration of the silica surface area during preparation of B4.5-RP (155 m^2/g catalyst). On the other hand, the surface area of the catalyst did increase from 155 to 267 m^2/g catalyst after a second impregnation of B4.5-RP with distilled water followed by drying at 110°C (B4.5-RP-W6-110).

Elemental analysis of the Cab-O-Sil fumed silica powder by inductively coupled plasma spectroscopy (ICP) showed Na, Al, and K present in the amounts of 63, 46, and 26 ppm, respectively. On the other hand, ICP of the water phase of a slurry of 20% by weight silica in water heated at 90°C for 12 h showed <2 ppm of Na, Al, and K. Thus, it can be concluded that these elements did not leach out of the silica significantly during the impregnation and/or drying processes.

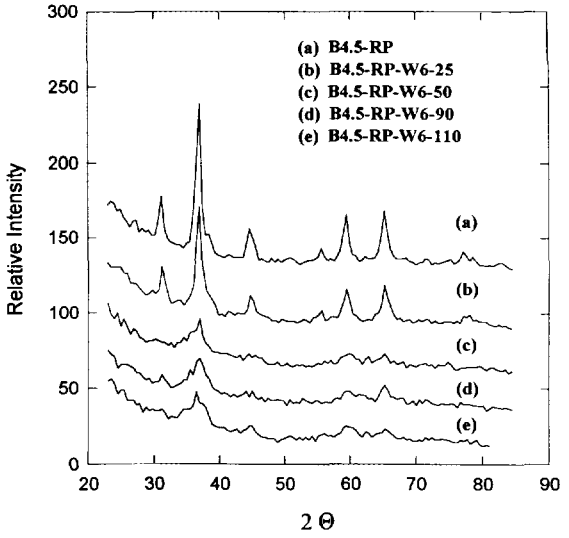

FIG. 1. XRD patterns for water-impregnated 20% Co/SiO_2 catalysts following drying at varying temperatures and calcining at 300°C: (a) B4.5, (b) B4.5-RP-W6-25, (c) B4.5-RP-W6-50, (d) B4.5-RP-W6-90, and (e) B4.5-RP-W6-110.

XRD

XRD patterns of the reduced and passivated base catalyst showed characteristic peaks corresponding to Co^0, Co_2O_3, and Co_3O_4 crystallites. The dominant phase was Co^0, having an average crystallite size of 9 nm, calculated using X-ray line broadening. On the other hand, XRD profiles of the water-impregnated and dried catalysts showed small broad peaks, indicating average crystallite sizes of ≤5 nm, the detectability limit of the technique. Recalcination was done to convert these phases into Co_3O_4 for better quantitative analysis of the Co phase. Figure 1 shows the XRD results of the base and water-impregnated reduced–passivated Co catalysts after recalcination. The XRD pattern of B4.5-RP corresponds to that of Co_3O_4. All the water-impregnated catalysts exhibited decreased amounts of detectable Co oxide crystalline phase as temperature of drying was increased to 50°C, after which there was little additional change. Table 1 shows the analysis of the XRD results performed on equal amounts of catalysts in order to permit quantitative analysis. While the decline in detectable crystallinity was about 25% for the catalyst dried at 25°C under vacuum, it was about 70% for the catalysts dried at the higher temperatures. Therefore, it emerges that H_2O impregnation plus drying has a pronounced effect on the detectable metal oxide crystalline phase after recalcination. The average Co oxide particle sizes of the base and impregnated reduced–passivated Co catalysts after recalcination are presented in Table 1. The Co_3O_4 crystallite size of B4.5-RP-W6-25 was relatively unchanged compared to the base catalyst. However, the cata-

TABLE 1

H_2 Chemisorption and XRD Results

Catalyst	H_2 chemisorption[a] (μmol H_2/g catalyst)		Avg. Co^0 d_p (after reduction)		Avg. Co_3O_4 d_p (recalcined) XRD (nm)	% Change detected by XRD in crystallinity of recalcined catalyst[c]
	Total	Irrev.	H.C. (nm)[b]	XRD (nm)		
B4.5-RP (20% Co/SiO_2)	88	70	13.5	9	15	0
B4.5-RP-W6-25	38	24	15	≤5	13	26
B4.5-RP-W6-50	—	—	—	≤5	11.6	70
B4.5-RP-W6-90	25	19	10	≤5	8	70
B4.5-RP-W6-110	41	39	6.6	≤5	6.6	70
B5-RP (20% Co/SiO_2)	60	47	20	—	27	0
B5-C-W6-90	54	40	22	—	24	0

[a] Static H_2 chemisorption at 100°C. Error estimated at ±10%.

[b] Estimated assuming $H_{total}/Co_s = 1$; S = metal surface area per gram of catalyst; $S = [Co_s] \times 5.46 \times 10^{-20}$ m^2, where Co_s = total number of Co^0 surface atoms per g catalyst = $H_{2,total} \times 2 \times N_{Avo}$; $d_p = 5/S_{Co}/\rho_{Co}$, where S_{Co} = Co surface area per gram Co^0 in catalyst = $S/\{0.2 \times (\%\ Co\ red.)\}$, ρ_{Co} = Co density; Based on % Co reduced during standard prereduction (see Table 2).

[c] Relative to B4.5-RP or B5-RP, using similar catalyst weights for measurements after preparation and calcination.

lysts dried at higher temperatures showed a significant decrease in average Co_3O_4 particle size with increasing drying temperature.

XRD results for the base catalysts B5-RP and B5-C-W6-90 (Table 1) show that, upon water impregnation and drying at 90°C of the recalcined base catalyst, little change was detected by XRD in the original properties.

TABLE 2

Reducibility Data

Catalyst	% Co reduced during TPR[a] to 900°C	% Co reduced during standard prereduction at 320°C[b]
B4.5-RP (20% Co/SiO_2)	85	85
B4.5-RP-W6-25	83	70
B4.5-RP-W6-50	55	8
B4.5-RP-W6-90	58	7
B4.5-RP-W6-110	64	13
B5-RP (20% Co/SiO_2)	86	86
B5-C-W6-90	87	87

[a] $Co_3O_4 + 4\ H_2 \rightarrow 3\ Co + 4\ H_2O$ for species reducing below 500°C, mol Co reduced = 3/4 (mol H_2 consumed); $Co_2SiO_4 + 2\ H_2 \rightarrow 2\ Co + SiO_2 + 2\ H_2O$ for species reducing from 500–900°C, mol Co reduced = mol H_2 consumed; % reduction = [(total mol Co reduced)/(total mol of Co)] × 100%. Error estimated at ±10%.

[b] Obtained from TPR 100–900°C after *in situ* reduction at 320°C for 12 h.

TPR

Table 2 presents the degrees of reduction during TPR of the recalcined catalysts. Figure 2 gives the TPR curves for the catalysts with water impregnation following reduction, passivation, and recalcination. The TPR profile for B4.5-RP in Fig. 2 shows two major reduction peaks at 280 and at 340°C, and a broad shoulder extending to 500°C. The first two peaks can be assigned to two different species of Co_3O_4, which reduce in two steps due to a bimodal distribution of Co_3O_4 crystallite sizes (19) and/or to different interactions with the support (14, 20). It has been reported that, when Co compounds are heated in air to >265°C, Co_3O_4 is formed (21). The broad shoulder peak is attributed to a Co^{3+} species interacting with the SiO_2 surface (19). For catalyst B4.5-RP-W6-25 dried under vacuum at 25°C, the Co_3O_4 peaks at 300 and 345°C decreased, and a new species reducible at 650°C appeared. For the catalysts dried at temperatures ≥50°C, the original Co_3O_4 peaks decreased almost completely, giving rise to a species primarily reducible only above 666°C. The reduction temperature peaks for this species for the catalysts dried at 50, 90, and 110°C were at 700, 778, and 778°C, respectively. Since the TPR experiment was carried out with a recalcination step, it was important to assess the effects, if any, of this recalcination step on the formation of the Co silicate. Thus, a TPR experiment on B4.5-RP-W6-90 was run without the recalcination step. The results of this latter experiment confirmed the existence of the species reducible only above 800°C, suggesting that it formed, or at least was initiated, during impregnation and drying. Base catalyst B4.5-RP had a reduction level of 85%. The total degree

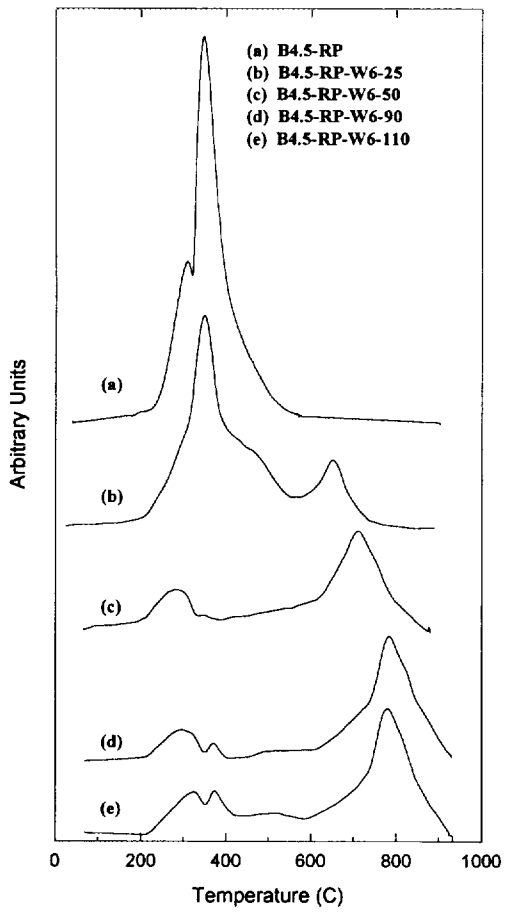

FIG. 2. Temperature-programmed reduction profiles for water impregnated 20% Co/SiO_2 catalysts following drying at varying temperatures: (a) B4.5, (b) B4.5-RP-W6-25, (c) B4.5-RP-W6-50, (d) B4.5-RP-W6-90, and (e) B4.5-RP-W6-110.

of reduction on TPR to 900°C was 83, 55, 58, and 64% for the catalysts dried at 25, 50, 90, and 110°C, respectively. It is therefore noted that, for reduced and passivated 20% Co/SiO_2, water impregnation and drying at or above 50°C led to ca. a 30% decrease in the degree of reduction of the Co. Table 2 also presents the degree of reduction based on the amount of Co reduced during reduction at 320°C, estimated by digital subtraction of the TPR profile of the catalyst signal after *in situ* rereduction at 320°C from the profile of a standard TPR of the calcined catalyst from 40–900°C. The degree of reduction during the standard reduction procedure (at 320°C) is more applicable for determination of the amount of Co^0 and its particle size for a catalyst as normally used. The performance of such calculations revealed reduction levels at 320°C of 85, 70, 8, 7, and 13%, respectively, for the base catalyst B4.5-RP and for the catalysts dried between 25 and 110°C. Figure 3 shows the TPR profiles of B4.5-RP-W6-90 for TPR from

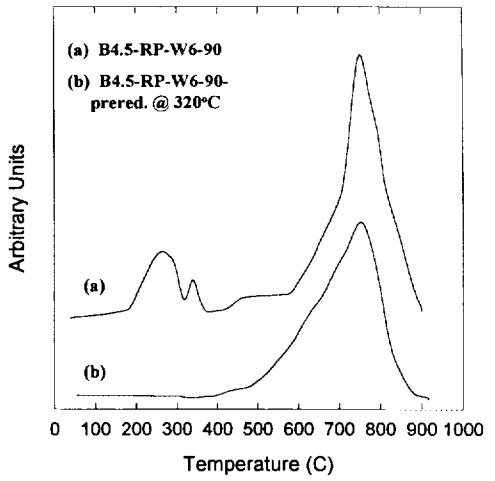

FIG. 3. Temperature-programmed reduction for B4.5-RP-W6-90 and for B4.5-RP-W6-90 after *in situ* reduction at 320°C for 12 h.

40–900°C and TPR after *in situ* reduction for 12 h at 320°C. These results indicate that the high-temperature species could not be reduced during the standard reduction treatment.

Figure 4 shows the TPR results for B5-RP-C, a base catalyst, and for B5-C-W6-90, the catalyst in which water impregnation was performed on the recalcined base catalyst (B5-RP-C). The reduction properties of B5-C-W6-90 were unchanged relative to the original catalyst B5 with all the Co_3O_4 peak characteristics being preserved. This indicates that water impregnation and drying of a calcined catalyst do not alter its reduction properties.

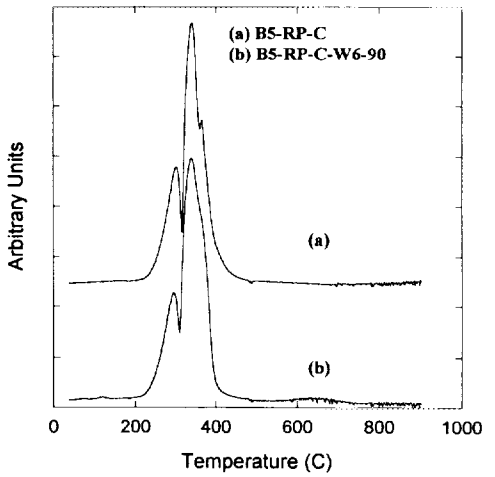

FIG. 4. Temperature-programmed reduction profiles for a calcined 20% Co/SiO_2 catalyst before and after water impregnation and drying at 90°C: (a) B5-RP-C, and (b) B5-RP-C-W6-90.

TABLE 3

Ethane Hydrogenolysis at 220°C

Catalyst	$R_{C_2H_6}$[a] (nmol/g/s)	TOF_H[b] $\times 10^3$	E_{app}[c] (kcal/mol)
B4.5-RP (20% Co/SiO_2)	38	0.22	23
B4.5-RP-W6-25	25	0.32	22
B4.5-RP-W6-50	26	—	24
B4.5-RP-W6-90	20	0.4	25
B4.5-RP-W6-110	22	0.26	21

[a] 220°C, 101 kPa, $H_2/C_2H_6/He$ = 15/0.3/84.7 cc/min. Error in rate measurements was ±8%.

[b] Based on H_2 chemisorption; TOF error estimated at ±20%.

[c] For reaction in the temperature range of 220–280°C.

Hydrogen Chemisorption

Table 1 presents the results of static H_2 chemisorption at 100°C on the 20% Co/SiO_2 catalysts before and after water impregnation and drying. These data show that the average Co crystallite size, d_p, of the base catalyst was 13.5 nm. Compared to the base catalyst, B4.5-RP-W6-25 showed no significant change in d_p while the catalysts dried at the higher temperatures showed decreasing values of d_p. These calculations were based on the total hydrogen uptake, which has been reported to more accurately represent the Co metal dispersion on silica (14), taking into account only the amount of Co reduced during the standard reduction procedure at 320°C. The total H_2 uptake for the unimpregnated catalyst, B4.5-RP, was about 88 μmol H_2/g catalyst. Table 1 shows, however, that there was more than a 50% decrease in total H_2 uptake after water impregnation. The total H_2 uptake was about 25–40 μmol H_2/g catalyst for all of these water-impregnated catalysts.

H_2 chemisorption data for B5-RP and for B5-C-W6-90 are also presented in Table 1. This technique also revealed that there was essentially no effect on the number of surface exposed Co^0 atoms, Co dispersion, or Co particle size when water impregnation was performed on a recalcined Co/SiO_2 catalyst.

Ethane Hydrogenolysis

Reactions were carried out on the water-impregnated reduced and passivated catalysts of this study between 220 and 280°C. Table 3 presents the ethane hydrogenolysis rates, the turnover frequencies, and the apparent activation energies for the catalysts at 220°C. A comparison of the activities of the water-impregnated catalysts with that of the unimpregnated base catalyst shows that the activities (per gram of catalyst) of the water-impregnated catalysts were 34–53% lower than that of the unimpregnated catalyst. The activation energy was essentially unchanged upon water impregnation and drying at the various temperatures. Based on the hydrogen chemisorption data, the TOF values increased with increasing temperature of drying to 90°C, and then decreased to a level still higher than that of the base unimpregnated catalyst for the catalyst dried at 110°C.

Reaction was not investigated for the water-impregnated calcined catalyst since it had manifested no XRD, H_2 chemisorption, or TPR differences from the unimpregnated base catalyst.

In order to develop a better picture of the surface activity of the catalysts, steady-state isotopic transient kinetic analysis of ethane hydrogenolysis was carried out for the base catalyst (B4.5-RP) and a water-impregnated catalyst (B4.5-RP-W6-90). SSITKA is a powerful kinetic technique for the determination of surface concentrations of active intermediates and their specific activities under steady-state reaction conditions. The water-impregnated sample chosen for this study was the one dried at 90°C. It represents a sample where all the changes accompanying water impregnation and drying were observed. The SSITKA results were evaluated based on a model developed by Chen and Goodwin using experimental measurements (18). According to this model, the reaction can be considered to proceed via two pools of surface intermediates in series. The first pool consists of intermediates, C_2H_x, and the second one consists of monocarbon species, CH_y. Using this model, the residence time (τ_i) of carbon-containing species on the surface, the concentrations of intermediates (N_j), and pseudo-first-order rate constants (k_j) can be determined from isotopic transients. k_1 is the activity of C–C bond rupture, and k_2 is that of the hydrogenation step. They both potentially contain the surface concentration of chemisorbed hydrogen. The SSITKA results (see Table 4) show that a measure of the true "TOF" of C–C bond rupture, k_1, more than doubled with distilled water impregnation and drying at 90°C. As can be noted in Table 4, the number of intermediates in pool 1 decreased from 2.5 to 0.5 μmol/g catalyst upon water impregnation and drying. This supports the TPR, XRD, and hydrogen chemisorption results that a sizable amount of the Co phase was converted into nonactive phases. The effects on the parameters of pool 2 were identical but less significant.

DISCUSSION

Water impregnation of a *reduced* and passivated Co/SiO_2 catalyst followed by drying at temperatures ranging from 25 to 110°C led to varying levels of interactions between the cobalt and the support. The 30% decrease in the degree of reduction for the catalysts dried at or above 50°C indicates the formation of a kind of CoO_x–SiO_2 phase that was not reducible during TPR. Room-temperature

TABLE 4

SSITKA of Ethane Hydrogenolysis at 260°C

Catalyst	$R_{C_2H_6}$[a] (μmol/g catalyst/s)	TOF_H[b] $\times 10^3$	$\tau_{C_2H_6}$ (s)	τ_{CH_4} (s)	τ_1[c] (s)	τ_2[c] (s)	k_1[c] (s^{-1})	k_2[c] (s^{-1})	N_1[c] (μmol/g catalyst)	N_2[c] (μmol/g catalyst)	Θ_1[b] $\times 10^2$	Θ_2[b] $\times 10^3$
B4.5 20% Co/SiO_2	0.4	2.3	0.76	1.4	0.76	0.64	0.16	1.52	2.5	0.26	1.4	1.5
B4.5-RP-W6-90	0.17	3.4	0.5	1.0	0.5	0.5	0.36	2.10	0.5	0.08	1	1.6

[a] At 260°C, 202.6 kPa, $H_2/C_2H_6/He$ = 6/0.15/43.85 cc/min.

[b] Based on static hydrogen chemisorption.

[c] k_j is the intrinsic activity of intermediates and N_j is the surface abundance of intermediates in pool one or two, based on the model developed by Chen and Goodwin (18): $\tau_1 = \tau_{C_2H_6}$, $\tau_2 = \tau_{CH_4} - \tau_{C_2H_6}$, $k_1 = R_{C_2H_6}/N_1$, $k_2 = 1/(\tau_{CH_4} - \tau_{C_2H_6})$, $N_1 = N_T - N_2$, $N_2 = R_{C_2H_6} \cdot \tau_2$, and where $N_T = R_{C_2H_6} \cdot t_{total}$ based on stopping the flow of ethane and measuring total surface intermediates reacted off under H_2.

drying after the impregnation step resulted in only moderate interactions. On the other hand, drying at higher temperatures (50, 90, and 110°C) resulted in almost total destruction of the Co^0 phase and produced a species completely reducible only above 700°C. In a study on the location of Ni and Ni oxide in silica-supported catalysts (25), two distinct types of "NiO" that reduce at different temperatures under TPR conditions were observed to form. The authors suggested that the more reducible oxide is present in the small pores, resembles bulk NiO, and has minimal interactions with the silica. The less reducible oxide was suggested to be either in the form of small crystallites or as surface nickel silicates which are present in the large pores. However, the silica used in our study is nonporous, suggesting that the Co phases we identify in our work could not be differentiated by distribution in different size pores of the support.

It has been reported that upon the direct heating of Co and silica the only phase which seems to form is the orthosilicate of Co ($2CoO \cdot SiO_2$) (21). Using high-surface-area silica, Puskas *et al.* (23) showed that supported Co would be converted completely to silicates if the pH of the Co precursor solution were around 8. They found by TPR that the cobalt silicate reduced at ca. 800°C. Okamoto *et al.* (19) prepared Co/SiO_2 catalysts from Co nitrate using the incipient wetness technique. Utilizing XPS and TPR, they found that several kinds of Co species formed on a Co/SiO_2 catalyst and assigned two of the species to Co^{3+} and to surface silicates (19). In both of these studies, Co silicates were formed during precursor solution impregnation because of the high pH. Ming and Baker (31) have also shown by XPS and TPR the formation of Co silicates or hydrosilicates during the initial preparation of Co/SiO_2 at pH's > 5 or after high-temperature calcination (ca. 1000°C). Recently, additional XPS evidence has been presented for the formation of Co silicates on Co/SiO_2 catalysts during preparation as a result of Co nitrate decomposition under vacuum conditions (32). Thus, there now exists quite a large volume of research identifying Co phases on Co/SiO_2 that are reducible only for temperatures >700°C as Co silicates or hydrosilicates. This leads us to conclude that the Co species formed in this study during secondary aqueous impregnation of prereduced Co/SiO_2 and reducible only above 700°C were Co silicates/hydrosilicates. Since the exact phase of such silicates is still not known and may in fact consist of several different species, these Co species will be referred to here as Co silicate/hydrosilicate to indicate that uncertainty.

The possibility of Co silicate/hydrosilicate formation during promoter addition in an aqueous solution having a lower pH has not been addressed. The pH of the aqueous solution used for secondary water impregnation in our study was 6, a value which can be considered close to the pH of the solutions used in the above studies. However, as our findings indicate, the pH of the aqueous solution was not the determining factor in the formation of Co silicate/hydrosilicate since the water-impregnated *calcined* catalyst (B5-C-W6-90) did not show any Co silicate/hydrosilicate formation. It appears that the state of the Co is a strong factor in the formation of the Co silicate/hydrosilicate during aqueous impregnation of *reduced* vs *calcined* Co/SiO_2. In addition, the temperature of drying appears to play a role.

Coenen (26) has studied a Ni/SiO_2 catalyst during reduction and has observed the occurrence of a hydrothermal treatment at higher water (from reduction) pressures, resulting in a lower degree of reduction and in increased Ni silicate formation. Thus, it is possible that even hydrothermal treatment during drying at 50–110°C of the catalysts containing *reduced* and passivated Co may have been able to initiate Co silicate/hydrosilicate formation. It is also possible that the net surface charge on the silica under these conditions played a role. Silica does not have a net surface charge, but in aqueous systems the surface of the silica particles will take on a charge dependent upon the pH of the system. At pH 2.3, Cab-O-Sil silica is at its isoelectric point, the pH at which its surface is neutral. As the pH is raised above the isoelectric point the surface

charge is increasingly more negative. By impregnating the catalyst with distilled water having a pH of 6, above the isoelectric point, the higher negative surface charge created may have resulted in stronger interactions between "reduced" Co and silica, leading to the formation of Co silicate/hydrosilicate. Considering that the reduced base catalyst was passivated before water impregnation, it is surprising that the presence of reduced Co behind the oxide barrier would result in Co silicate/hydrosilicate formation, although all the evidence supports this conclusion.

Puskas *et al.* (23) have shown the surface area of the silica to be a strong factor in the formation of Co silicate. The structure of the silica support used in this study consisted of three-dimensional, chain-like aggregates of fused silica particles that entangle, forming agglomerates. A basic difference between the original impregnation of the precursor solution onto the silica and that of distilled water impregnation of the reduced and passivated Co catalyst was the pH, 4.5 vs 6, respectively. The second impregnation resulted in an increase in the overall surface area of the catalyst. This was surprising to us since usually quite the opposite occurs. However, this impregnation was performed at the higher solution pH of 6. At this pH, the negative charge induced on the silica was possibly sufficient to generate sufficient electrostatic repulsion for the silica particles to be separated to a greater extent, thereby producing the higher surface area observed. The other possibility is that the formation of Co silicate/hydrosilicate may have altered the morphology of the silica particle, leading to the higher surface area (27).

The broad TPR peaks observed, the decreased amount of Co reducible during reduction at 320°C, and the smaller Co oxide particles observed by XRD indicate variation in the dispersion of the Co phase upon impregnation and drying. Coenen (26) suggested that the Ni silicate formed during precursor impregnation could act as a bonding layer between the support and the hydroxide/oxide/metal through an epitaxial relationship. He concluded that the silicate, by inhibiting sintering, aided the formation and retention of small crystals of the oxide and of the metal.

As mentioned before, ethane hydrogenolysis is well known to be structure sensitive. The effect of metal dispersion on ethane hydrogenolysis activity has been thoroughly investigated (28, 29). In those studies of supported Ni and Rh catalysts, the specific activities of the catalysts increased 10-fold for a decrease in crystallite size from 6 to 3 nm. The TOF value of ethane hydrogenolysis measured at 220°C increased with increasing drying temperature to 90°C, above that temperature for the 110°C dried catalyst it decreased but was still higher than that of the base catalyst. For the 110°C dried catalyst, the drying temperature being above the boiling point of water may have led to a lower contact time between the water and the catalyst, producing different effects on the catalyst activity. On the other hand,

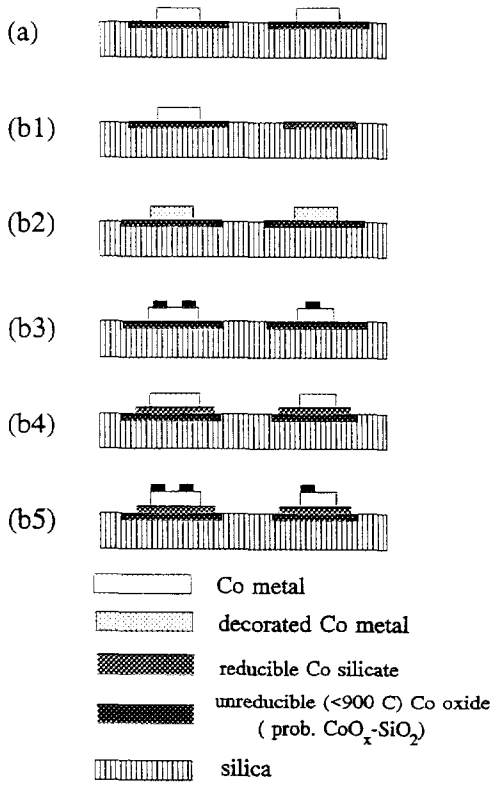

FIG. 5. Schematic of catalyst surface before and after water impregnation and drying.

SSITKA of ethane hydrogenolysis performed at 260°C also showed an intrinsic rate (true TOF) for the catalyst dried at 90°C double that of the base catalyst. Thus, it has been shown by two independent experiments that the catalyst dried at 90°C has more than double the TOF of the unimpregnated base catalyst. Since XRD and H_2 chemisorption results support the formation of smaller particles with water impregnation and drying at 90°C, the higher TOF observed is attributed to the decrease in the particle size.

Five possible models can be proposed to represent the Co/SiO_2 catalyst surface after water impregnation of the reduced and passivated catalyst. These five models and a model of the catalyst before water impregnation are discussed in detail below and are shown in Fig. 5. Model (a) shows that, before impregnation, the reduced catalyst surface probably consisted of Co metal particles on top of a CoO_x–SiO_2 phase. The presence of a CoO_x–SiO_2 phase was indicated by the incomplete reduction (85%) of the base catalyst during TPR to 900°C.

The models (b_i) represent possible situations which might exist after H_2O impregnation and pretreatment of the reduced and passivated catalyst. Model (b1) shows a situation where the Co silicate/hydrosilicate formed was isolated from the Co particles. Model (b2) presents the

possibility that Co silicate/hydrosilicate, formed during water impregnation and drying, was dispersed over the Co metal particles. Model (b3) shows Co silicate/hydrosilicate dispersed in large patches over the Co metal particles, and model (b4) shows a situation where a smaller Co particle phase is produced on top of a thin Co silicate/hydrosilicate layer and a CoO_x–SiO_2 phase.

Model (b1) is not likely since Co silicate/hydrosilicate should be formed at the Co–SiO_2 interface. Based on the results for ethane hydrogenolysis, which requires an ensemble size of ca. 12 metal atoms per reaction site (9), model (b2) seems unlikely since such an occurrence would be expected to lead to a greater decline in reaction rates than was observed. This is especially true since the amount of Co silicate/hydrosilicate formed was very significant according to TPR and XRD measurements. However, the fact that a significant amount of Co silicate/hydrosilicate was formed yet no Co silicate/hydrosilicate phase was detected by XRD would imply that it existed either in very thin layers or as small particles (<5 nm in diameter). Model (b3) represents the case where thin islands of Co silicate/hydrosilicate exist on the Co metal surfaces, while model (b4) presents the situation where the Co silicate/hydrosilicate lies under the Co^0 particles due to strong interactions with the support. Model (b5) represents a combination of models (b3) and (b4).

XRD and H_2 chemisorption showed, in fact, smaller crystallite sizes of Co_3O_4 and Co metal for the catalysts dried at higher temperatures. SSITKA results for ethane hydrogenolysis also showed average higher intrinsic activities of the same catalysts, which were attributed to smaller metal particle sizes. Stronger metal–support interactions were indicated by the broad TPR peaks. Since it would be expected that Co silicate/hydrosilicate would lie at the Co–SiO_2 interface, model (b4) or, possibly, model (b5) appears to explain best the experimental results.

This study presented evidence for the formation of two Co–SiO_2 phases upon water impregnation and drying, a reducible Co silicate/hydrosilicate phase and a nonreducible phase identified here only as unreducible (<900°C) CoO_x–SiO_2. The nonreducibility of the second phase could be due to its having a different structure.

CONCLUSIONS

Water impregnation and drying of a *reduced* and passivated Co/SiO_2 catalyst result in conversion of sizable amounts of the Co phase into Co silicate/hydrosilicate. On the other hand, when water impregnation and drying are performed on a *recalcined* catalyst, no detectable changes in the catalyst structure or reduction properties are observed. The Co silicate/hydrosilicate formed in the earlier case is unable to reduce during the standard prereduction. The formation of Co silicate/hydrosilicate is explained in terms of a hydrothermal treatment during drying, leading to Co silicate/hydrosilicate. Recent results (30) indicate that the Co silicate/hydrosilicate formation is not a strong function of pH of H_2O impregnation, although in that study a different grade silica was used. Drying temperature, however, has a pronounced effect on the level of metal–support interactions. Drying above 50°C leads to a significantly lower degree of reduction of the Co phase and to an increase in the reduction temperature of the Co silicate/hydrosilicate. An increase in the support surface area due to the breakup of the three-dimensional silica structure is suggested to have aided in Co silicate/hydrosilicate formation. A model of the water-impregnated *reduced* catalysts is put forward. It shows smaller Co metal particles dispersed on top of a Co_3O_4/Co silicate base.

Finally, this work suggests the type of complications which may occur during the addition of a promoter to a catalyst and which can obscure the true effect of the promoter.

ACKNOWLEDGMENTS

The authors thank Amoco Oil Co. and N.S.F. (Grant CTS-9102960) for financial support.

REFERENCES

1. Iyagba, E. T., Hoost, E., Nwalor, J. U., and Goodwin, J. G., Jr., *J. Catal.* **123,** 111 (1990).
2. Ponec, V., *in* "Metal–Support and Metal–Additive Effects in Catalysis" (B. Imelik *et al.*, Eds.), p. 63. Elsevier, Amsterdam, 1982.
3. Mross, W. D., *Catal. Rev. Sci. Eng.* **25,** 591 (1983).
4. Barrault, J., Guilleminot, A., Achard, J. C., Paul-Boncour, V., and Percheron-Guegan, A., *Appl. Catal.* **21,** 307 (1986).
5. Hoek, A., Joustra, A. H., Minderhoud, J. K., and Post, M. F., UK Patent Application GB 2-123-062 A, 1986.
6. Post, M. F. M., and Sie, S. T., European Patent Application 0 167 215, 1985.
7. Goodman, D. W., *Surf. Sci.* **123,** L679 (1982).
8. Martin, G. A., *J. Catal.* **60,** 345 (1979).
9. Martin, G. A., *Catal. Rev. Sci. Eng.* **30,** 519 (1988).
10. Sinfelt, J. H., *Catal. Rev. Sci. Eng.* **3,** 175 (1969).
11. Ko, E. I., Hupp, J. M., and Wagner, N. J., *J. Catal.* **86,** 315 (1984).
12. Gallaher, G. R., Goodwin, J. G., Jr., and Guczi, L., *Appl. Catal.* **73,** 1 (1991).
13. Hoost, E. T., and Goodwin, J. G., Jr., *J. Catal.* **130,** 283 (1991).
14. Reuel, R. C., and Bartholomew, C. H., *J. Catal.* **85,** 63 (1984).
15. Zowtiak, J. M., and Bartholomew, C. H., *J. Catal.* **83,** 107 (1983).
16. Happel, J., *Chem. Eng. Sci.* **33,** 1567 (1978).
17. Biloen, P., *J. Mol. Catal.* **21,** 17 (1983).
18. Chen, B., and Goodwin, J. G., Jr., *J. Catal.* **154,** 1 (1995).
19. Okamoto, Y., Nagata, K., Adachi, T., Imanaka, T., Inamura, K., and Takyu, T., *J. Phys. Chem.* **95,** 310 (1991).
20. Lapidus, A., Krylova, A., Kazanskii, V., Borovkov, V., and Zaitsev, A., *Appl. Catal.* **73,** 65 (1991).
21. Young, R. S., "Cobalt: Its Chemistry, Metallurgy, and Uses," p. 78. Reinhold, New York, 1961.
22. Roe, G. M., Kidd, M. J., Cavell, K. J., and Larkins, F. P., *in* "Proceedings of a Symposium on the Production of Fuels and Chemicals from Natural Gas, Auckland, April 27–30, 1987," Studies in Surface Science and Catalysis, Vol. 36, Methane Conversion, p. 509. Elsevier, Amsterdam, 1988.

23. Puskas, I., Fleisch, T. H., Hall, J. B., Meyers, B. L., and Roginski, R. T., *J. Catal.* **134,** 615 (1992).
24. Gmelins Handbuch der Anorg. Chemie: Kobalt, Vol. 58, p. 735. Verlag Chemie, Weinheim, 1961.
25. Mile, B., Stirling, D., Zammitt, M. A., Lovell, A., and Webb, M., *J. Catal.* **114,** 217 (1988).
26. Coenen, J. W. E., *in* "Preparation of Catalysts II" (B. Delmon, P. Grange, P. A. Jacobs, and G. Poncelet, Eds.), p. 89. Elsevier, Amsterdam, 1979.
27. Lin, B., Cabot Corporation Cab-O-Sil Division, private communication.
28. Carter, J. L., Cusumano, J. A., and Sinfelt, J. H., *J. Phys. Chem.* **70,** 2257 (1982).
29. Yates, D. J. C., and Sinfelt, J. H., *J. Catal.* **8,** 348 (1967).
30. Weber, J., Kogelbauer, A., and Goodwin, J. G., Jr., *Catal. Lett.*, in press (1995).
31. Ming, H., and Baker, B. G., *Appl. Catal. A.* **123,** 23 (1995).
32. Coulter, K. E., and Sault, A. G., *J. Catal.* **154,** 56 (1995).